Quantifying Roll Feel of a Car by Using a Musculoskeletal Mathematical Model

Masaki Izawa[1], Ryota Araki[1], Tatsuro Suzuki[1], Kaito Watanabe[2] and Kazuhito Misaji[3, *]

Abstract: Primary purpose of this research is to create a three-dimensional musculoskeletal mathematical model of a driver of a car using a motion capture system. The model is then used in an analysis of drive torque around joints and attached muscles as a vehicle travels in different travel modes and damping force settings to examine 'burdens' for the driver. Previous studies proposed a method of quantifying the degree of musculoskeletal load in simple human motion from the changes in drive torque around joints and attached muscles. However, examination of the level of burdens for the driver while driving using this method does not seem to exist. Especially within the scope of evaluating different travel modes and dampers, there is no other study. Results of this study are hence a valuable new perspective on quantitative analysis of the burdens for the driver's joints and muscles depending on the different settings of travel modes and dampers.

1 Introduction

Popularity of cars vastly affected our society to enrich our lives as they became ubiquitous. In Japan, more than one vehicle per household was registered in 1996 [Automobile Inspection & Registration Information Association (2017)] and it is something 'anyone can have' since-with the consequence of changing demands of users. A recent study in Japan reveals that users demand driving comfort as well as good performance of a car; namely 'easy handling', 'ride comfort', 'safety/sense of security', 'fuel efficiency' and 'style/design' [Cross-Marketing (2017)].

There are different approaches to improve driving comfort. One is to reduce noise and vibration, the other is to enhance smooth 'roll feel' registered by the driver at the corner. For the former, it is common to apply vibration theory and there are various technologies used in mass production e.g., use of vibration-proof materials to reduce the noise level, as well as controlling vertical vibration as a seminal study done by Karnopp et al. [Karnopp,

---

[1] Showa Corporation, 112-1 Haga-dai, Haga-mach, Haga-gun, Tochigi, Japan.

[2] Ex-Graduate Student, Nihon University, College of Industrial Technology, Department of Mathematical Information Engineering, Japan.

[3] Nihon University, College of Industrial Technology, Department of Mathematical Information Engineering, Japan.

* Corresponding Author: Kazuhito Misaji. Email: misaji.kazuhito@nihon-u.ac.jp.

Crosby and Harwood (1974)]. In terms of the roll feel evaluation, it is inequivalent in a way that roll feel is a combination of assessment on handling and reception of the roll feel (sensory evaluation). This topic has been broadly attracting attention of automotive engineers to explain the mechanism such as research on the phase portrait between roll rate and pitch rate examined in association with physical value of a car and sensory evaluation, studies on relationships between physical value of a car and surface EMG, brain waves and sensory evaluation of roll feel using biological indexes [Tao, Sugimacgi, Suda et al. (2016); Yoshioka, Abe, Yamakado et al. (2017)].

These researches indicate the difficulty of showing an evidence of associations between biological indexes e.g. EMG/EEG and sensory evaluation of roll feel, resulting in statistical treatment upon examination of objective appraisal of roll feel involving physical value of a car, biological indexes and sensory evaluation.

The authors thus felt it was sensible to introduce a musculoskeletal mathematical model in quantification technique evaluating muscle load of a driver while controlling a vehicle in quantification of roll feel.

In quantification studies of muscles and joint load during exercise, it is common to analyze a three-dimensional musculoskeletal model using motion capture data [Watanabe, Izawa, Misaji et al. (2018)]. Ride comfort related musculoskeletal research, however, are mainly conducted by collecting data measured in a driving simulator rather than data during driving on the road [Ogabayashi (2010)]. In this study, data of the driver's posture was recorded while driving using motion capture cameras in creation of a three-dimensional musculoskeletal model, so that we could quantitatively analyze the load on muscles and joints by examining the changes of drive torque's time series data and muscle activity level, which is a conventional analytical method.

Load of the driver's body while driving could be quantified by analyzing these results in order to quantitatively compare the difference in roll feel caused by the driving modes and damper variations.

2 Analysis method

2.1 Rigid body link model (skeleton model)

Reflective markers were affixed to the physique of the subject and photographed using the motion-capture camera. In that way, the position of each reflective marker could be acquired as three-dimensional coordinate data. By labelling each of the obtained three-dimensional coordinate data and defining links between the points as a rigid body, a "rigid-body link model" matching the physique of the subject was created as shown in Fig. 1. The posture of each segment and the angle of each joint from the three-dimensional coordinate data was calculated using inverse kinematics calculation to this model. Cortex from Motion Analysis was used for these calculations.

2.2 Musculoskeletal mathematical model

The rigid body link model (Fig. 1) shows a model of the motion measurements by motion captures. The musculoskeltal model (Fig. 2) is a model of a muscle-tendon complex consisting of muscle fibers and tendon tissues. Based on this individual rigid body link

model of each subject a musculoskeletal mathematical model is created, which is scaled to the subject's body. Thus, musculoskeletal mathematical model is a model of muscle tendon complex that integrates muscle fibers and tendon tissues.

Muscles in the muscle-tendon complex are composed of "active contractile elements" (CEs), which actively exert force by muscle contraction-commonly called "agonist muscle"-and "parallel elastic elements" (PEEs), which exert force as an elastic body passively elongated by muscle contraction - commonly called "antagonist muscle". On the other hand, tendons are passively extended by muscle contraction and exert force as an elastic body, so they are called "serial elastic elements" (SEE). As for the musculoskeletal mathematical model used in this study, we used the model proposed by Zajac [Zajac (1989)] based on the Hill-type model proposed by Hill [Hill (1938)] (Fig. 3). As shown in Fig. 4, the model proposed by Zajac [Zajac (1989)] clearly expresses relationships between extension and tension, muscle length and tension, and muscle speed and tension of a series of elastic elements expressing the mechanical properties of muscles and tendons. Motion-analysis software   SIMM (Motion Analysis) was used for the analysis of these relationships.
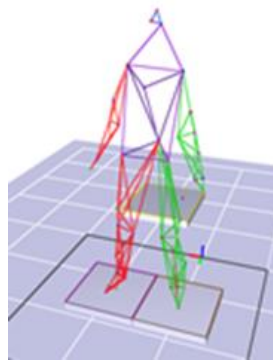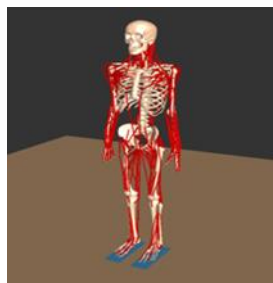

Figure 1: Rigid-body-link model
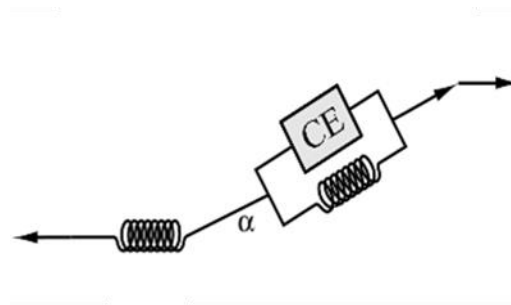

Figure 2: Musculoskeletal model

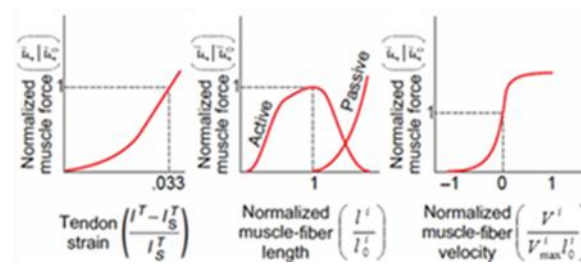**Figure 3:** Hill type model

Figure 4: Mechanical properties of any muscle and tendon in the body

2.3 Inverse kinematics calculation

As for the inverse-kinematics calculation using the rigid-body link model, each joint angle can be acquired by the measured three-dimensional coordinate data and physique information such as height and weight. A schematic diagram of the knee joint during an extension movement is shown in Fig. 5 as an example.
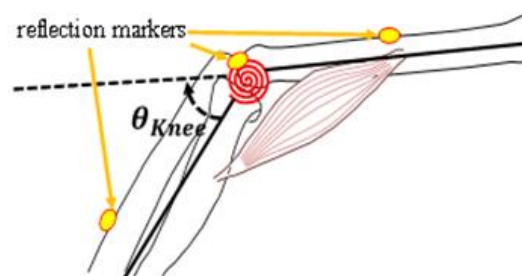

Figure 5: Driving torque around knee joint

The knee-joint angle is given as θ_{knee} in Fig. 5. θ_{knee} can be calculated by converting the positions of reflection markers fixed to the center of rotation of the knee joint and reflection markers fixed to the thighs and lower legs (captured by amotion-capture camera) into three-dimensional coordinate data.

2.4 Inverse dynamics calculation

As for the inverse-dynamics calculation, by using the musculoskeletal mathematical model, the degree of muscle activity is estimated from each joint angle (calculated from the inverse kinematics calculation) and the driving torque around each joint (calculated from the three-dimensional coordinates of each segment). The driving torque around each muscle in the joint can then be obtained. As an example, a schematic diagram of the extension movement of the knee joint is shown in Fig. 6.
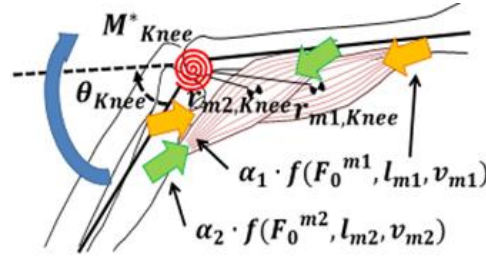

Figure 6: Muscle torque around the knee joint

In this figure, α_i is muscle activity in the i-th muscle, $f(F_0^i, l_i, v_i)$ is a function of the i-th muscle shown in Fig. 3 and the maximum isometric contraction force, and $r_{i,j}$ indicates moment arm length of the i-th muscle for around the j-th joint. The product of the muscle activity level of the i-th muscle and the mechanical property of the i-th muscle is the muscular strength of the i-th muscle. Further, by taking the product of that value and the moment arm length of the i-th muscle, the muscle torque of the i-th muscle can be acquired. The equation for calculating muscle torque $M_{i,j}$ of the i-th muscle is given as

$$M_{i,j} = a_i \cdot f(F_0^i, l_i, v_i) \cdot r_{i,j} \tag{1}$$

Also, the sum of the driving torques around the j-th joint and the sum of the driving torques around the i-th muscle in the j-th joint (calculated by the inverse dynamics calculation) are counter-balanced, hence Eq. (2) is derived as

$$\sum_{i=1}^{n} \{ a_i \cdot f(F_0^i, l_i, v_i) \} r_{i,j} = M_j^* \tag{2}$$

Here, $f(F_0^i, l_i, v_i)$, $r_{i,j}$ is a known value and α_i is an unknown value, so muscle activity level α_i in the i-th muscle can be estimated by performing an optimization calculation using the least squares method. The outer-muscle potential can be measured by using an electromyograph. It is used as a guide for estimating the muscle activity level of a muscle by normalizing the measured myoelectric potential with the maximum muscle force. By applying estimated muscle activity level α_i in the i-th muscle in Eq. (1), muscle torque $M_{i,j}$ of the i-th muscle can be obtained.

3 Experimental method

3.1 Three-dimensional position coordinate data measurement

Six motion-capture cameras were installed in the interior of a test car. Thirty-two

reflection markers and six electromyographs were affixed to the upper body of the subject (male, 31 years old, height: 175 cm; weight: 66 kg) and static data was measured to create a rigid-body link model suitable for the subject's physique.

Next, motion data, was measured by recording the data during the subject drove the car. In addition to the motion capture cameras, a gyro sensor and a steering force meter were installed inside the car to measure the behavior of the car and the steering reaction force. Fig. 7 and Fig. 8 show the positions of the cameras and the experiment environment.
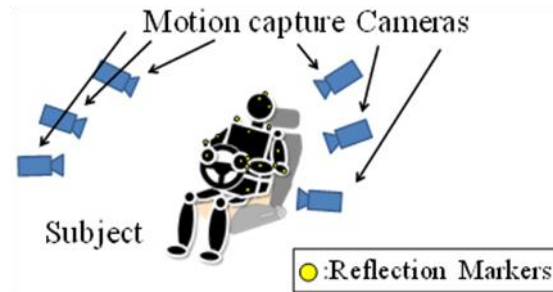

Figure 7: Outline of measurement set up

Figure 8: Motion capture installation

The test car was run in three modes: "vehicle sine-slalom", "steering-angle sine-slalom" and "line trace". The above-described measurements were carried out twice in each running mode. The car used for this test had a set of variable dampers, described in detail in the following chapter fitted, which allowed measurement switching between "comfort mode" and "sports mode".

3.2 Variable damper system

It is known that vertical vibration of a vehicle caused by the input of the road surface disturbance (fluctuation of vehicle's steadiness) is affected by the variation in the magnitude of the damping force. When damping force is large, sprung mass resonance is suppressed, but the vibration transmission in the frequency region (i.e., transmission region) between the sprung mass resonance and the unsprung mass resonance increases. On the contrary, when the damping force is small, the damping effect of the sprung mass resonance becomes lower, yet the vibration in the transmission region decreases. This

results in drivers' preference on setting with small damping force (i.e., comfort mode) as to the variable dampers' setting when they desire comfortable driving feeling; on the other hand, when they desire nimble driving feeling, they prefer large damping force (i.e., sport mode). Similar practice can be seen for roll behavior during steering too. Fig. 9 is an example of qualitative analysis showing roll angular velocity, roll angle at the time of step steering and gain of the Bode diagram corresponding to each vehicle state.

comfort: C2=1600 [Ns/m]

sport: C2=4500 [Ns/m]

Calculation was done using the model given in Vehicle Behavior Analysis Using Linearization Method of Nonlinear Vehicle Equations of Motion [Izawa, Kageyama, Misaji et al. (2017)] with C2 as damping coefficient. The results show the convergence of roll in comfort mode is worse than that in sport mode.
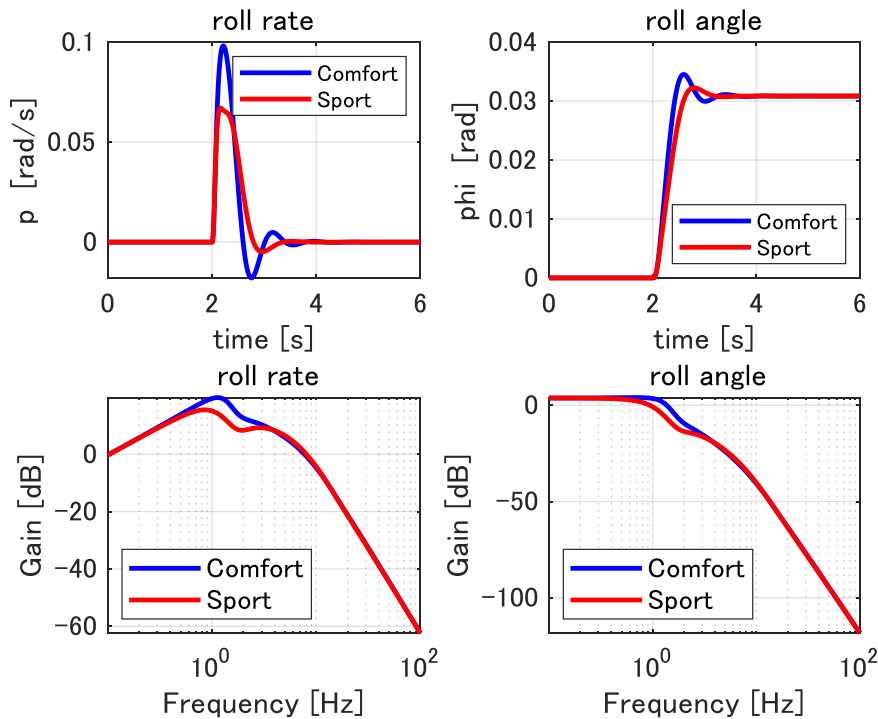

Figure 9: Vehicle roll behavior

The measured roll angular velocities in comfort and sport modes during slalom running of an actual vehicle test are shown in Fig. 10. While the variances may look small, it is apparent that roll angular velocity has poorer convergence in comfort mode than in sport mode, which is consistent with the drivers' comments. As for lateral acceleration of the car, no significant differences between comfort mode and sport mode are apparent. It can be assumed this is resulted by the tire lateral force generated by the steering input being hardly affected by the variation of damping force. These observations let us conclude that although the roll rate of the car (i.e., attitude of the car) changes in different driving

modes (i.e., different damping forces), the lateral force received by the vehicle does not.
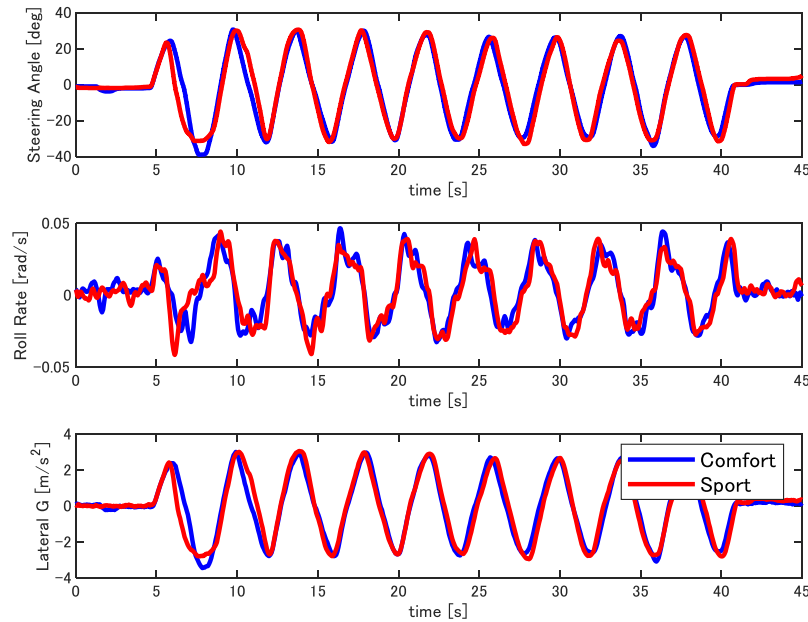

Figure 10: Roll behavior of vehicle performing slalom motion

3.3 Muscle activity level measurement

Six surface electromyographs (MQ-Air: manufactured by Kissei Comtech Co., Ltd.) were attached to the outer muscles; left and right sternocleidomastoid muscles, deltoid muscles (clavicular portion) and long palmar muscles, which are considered as significantly contributing to driving a car, to measure the myoelectric potential. Based on the action of each muscle [Sakai (2011)], the myoelectric potential at the time of maximum isometric muscle force was measured and used to normalize the myoelectric potential measured as the subject was driving the car. Fig. 11 and Fig. 12 illustrate the positions of the electromyograph and reflection markers affixed to the subject. Fig. 13 shows the interior of the car during the examination.
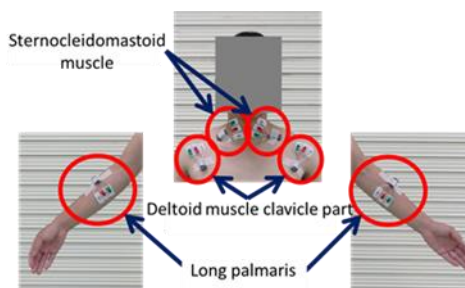

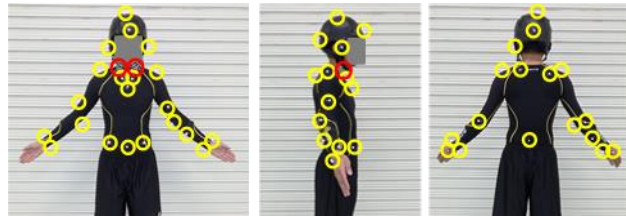**Figure 11:** Attachment of an electromyograph to a subject

Figure 12: Position of reflection markers and EMG

Figure 13: Interior of the cabin during measurement

4 Driving modes

4.1 Sine slalom driving in comfort mode

The variable dampers of the car were set to comfort mode and the car drove sineslalom. The "sine slalom" in this study is a set-up in which the car is driven by the steering operation in a manner that its traveling locus draws a sine curve as viewed from above. The measurement conditions were vehicle speed of 80 km/h, steering angle of 25 degrees and steering cycle of 0.1 Hz.

4.2 Sine slalom driving in sport mode

The variable dampers of the test car were set to sport mode and the car drove sine slalom. The measurement conditions were the same as above; vehicle speed of 80 km/h, steering angle of 25 degrees and steering cycle of 0.1 Hz.

5 Analysis musculoskeletal mathematical model construction

5.1 Musculoskeletal mathematical model construction

The rigid link model and the muscle activity level calculated from the measured myoelectric potential were used to construct an upper-body musculoskeletal mathematical model, which was scaled to the physique of the subject as shown in Fig. 14
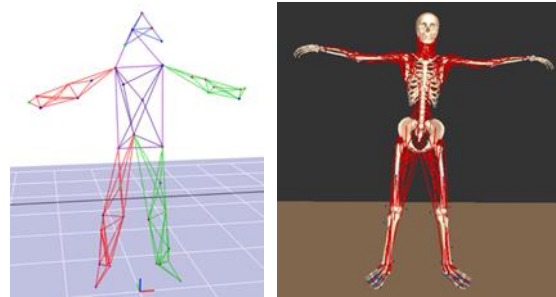
Figure 14: Model scaled to the physique of the subject. a (left): rigid link model, b (right): musculoskeletal model

5.2 Accuracy verification

As for verifying the accuracy of the musculoskeletal mathematical model, from the motion data captured by the motion capture cameras, sum totals of the drive torque around each joint (obtained by the inverse kinematics calculation) and the drive torque around each muscle in each joint (calculated from Eq. (1)) were compared. The verification results concerning the accuracy of the model for determining torques exerted in the neck joint during lateral bending motion are shown in Fig. 15.
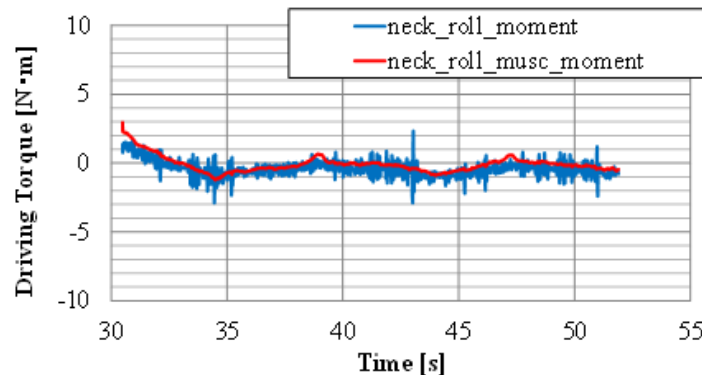

Figure 15: Torques exerted on neck joint during lateral bending motion

According to Fig. 15, the sums of the drive torque around the neck joint (obtained through inverse kinematics calculation) and the drive torque around each muscle in the neck joint (calculated from Eq. (1)) are almost identical. The accuracy of the analysis by the three-dimensional musculoskeletal mathematical model is thus considered sufficient.

6 Analysis and considerations

In this chapter, various comparisons are presented to analyse different types of burden, namely comparisons of driving torques with different vehicle dampers in comfort and sport modes as the car drove sine slalom. In the analysis, the steering action was divided into left steering and right steering.

6.1 Burden analysis on joints

Drive torques during side bending motion, rotation motion and bending motion of the neck joint in comfort and sport modes during left steering (calculated using the inverse kinematics calculation) are shown in Figs. 16 to 18, respectively.
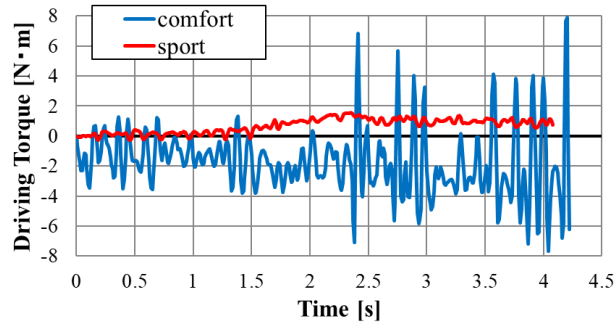
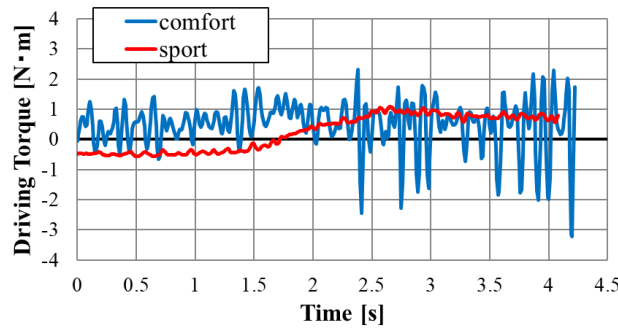**Figure 16:** Comparison of driving torques on neck joint during lateral bending motion as steering left

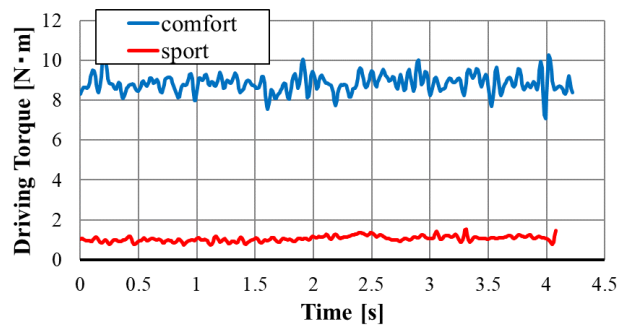**Figure 17:** Comparison of driving torques on neck joint during rotation motion as steering left

Figure 18: Comparison of driving torques on neck joint during bending forward motion as steering left

Above observation on the motion around the neck joint reveals that change in the drive torque with time is severe in comfort mode, whereas it is small in sport mode. Moreover, Fig. 18 indicates driving torque in comfort mode is about nine times larger than that in sport mode. These analysis results concerning change in driving torque around the neck joint with time leads us a conclusion that sport mode is more stable than comfort mode in sine slalom.

6.2 Burden analysis on muscle

The neck muscles analyzed in this study are shown in Fig. 19. It is known that driver unconsciously compensates the force felt during cornering by supporting their tilting body to keep their heads vertically.
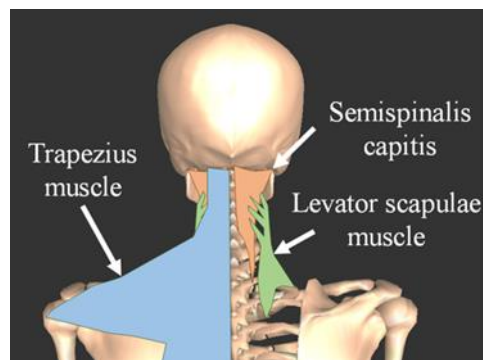

Figure 19: Muscles around the neck

In case of animals, there is an analysis example of locomotion research showing movements of a cheetah hunting at high speed keeping its body axis level [Wada (2012)]. Inspired by these facts, our focus was those three muscles around the neck from the viewpoint of the burden on the body to suppress the change in the posture of the head corresponding to the car's rolling motion; considering the "definition of shoulder stiffness" given in a medical dictionary [Sasaki (1994)]. Figs. 20 to 22 show driving torques of the left trapezius muscle, left shoulder levator scapulae muscle and left head semispinalis capitis muscle on the side of the neck joint in comfort and sport modes during left steering, calculated from Eq. (1).
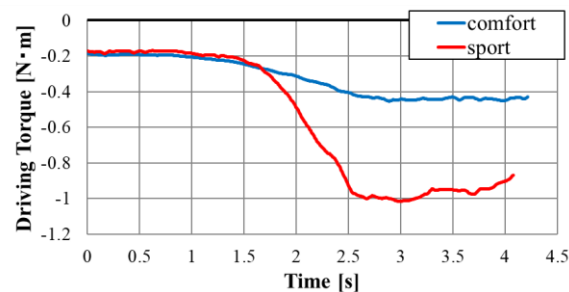

Figure 20: Comparison of driving torques around trapezius muscle on neck joint
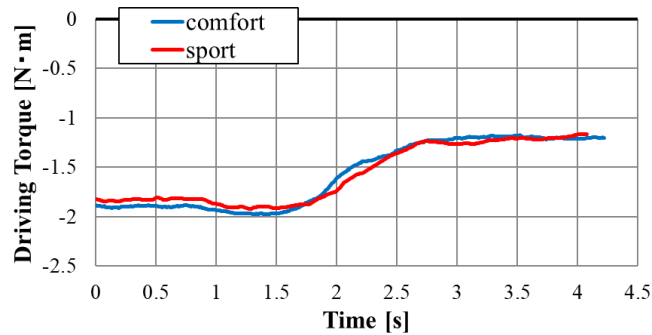
Figure 21: Comparison of driving torques around levator scapulae muscle on neck joint
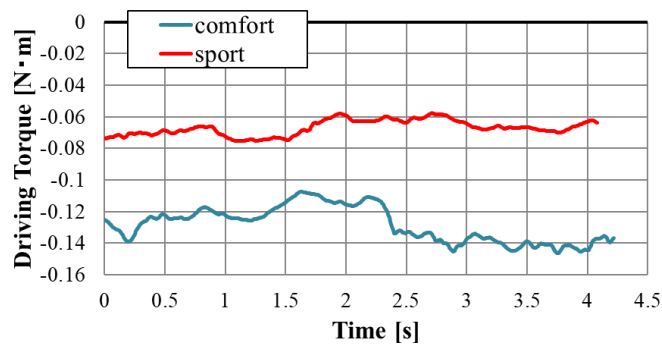

Figure 22: Comparison of driving torques around semispinalis capitis muscle on neck joint

According to Fig. 20, the driving torques of the left trapezius muscle agree closely at the beginning of the operation; however, as the left-steering maneuver continues, the driving torque in sport mode becomes about 2.3 times larger than that in comfort mode. According to Fig. 21, the driving torques on the left shoulder levator scapulae muscle agree closely throughout the maneuver. According to Fig. 22, the driving torque on the left head semispinalis capitis muscle in comfort mode is about 2.2 times larger than that in sport mode. From the relationships between the analysis results for driving torque on each muscle in the neck joint and the muscle attachment position, it is clear that during left steering, the muscle tension around the shoulder increases in sport mode, but the muscle tension around the neck joint increases in comfort mode.

7 Conclusion

We can draw following conclusions:

1. Creation of a valid musculoskeletal mathematical model of a driver while controlling a vehicle was enabled through a motion capture system used to examine inside the car.

2. Our analysis of the time series data of drive torque around the neck joints indicates more stable driving is realized in sport mode compared to comfort mode.

3. Our analysis of the time series data of drive torque around the neck muscles reveals less load in comfort mode compared to sport mode.

4. Our observation shows it is easier for the driver to control the vehicle when an appropriate rolling posture is realized. Assuming the same lateral force as the traveling vehicle is received by the driver at the corner, it is easier to keep the posture in sport mode as there is less drive torque around the neck joints and the driver can counter the force by increasing the muscle load.

5. In this study, a musculoskeletal mathematical model was created and analyzed for the upper body only. Yet the driver's body is presumably supported by other body parts i.e. back by the back upholstery, thighs by the seat and feet by the floor; hence analysis of the entire body is planned next using force plates attached to the seat and the floor of a car to measure the reaction force, which was prohibited this time because of the lack of plates in suitable sizes.

We consider it is reasonable to quantitatively analyze a car's ride comfort during travel with physical quantities viably by examining the changes of drive torque's time series data. Also, it is believed there is an appropriate rolling posture for a car to make it easy for the driver to control. These findings were worthwhile upon engineering better roll feel to be experienced by drivers.

References

Automobile Inspection & Registration Information Association (2017): Latest automobile ownership survey. https://www.airia.or.jp/publish/statistics/number.html.

Cross-marketing Co., Ltd. (2017): Actual condition survey on automobiles. https://www.cross-m.co.jp/_file/ja/article/1331/pdf/.

Hill, A. V. (1938): The heat of shortening and the dynamic constants of muscle. *Proceedings of the Royal Society*, vol. 126, pp. 136-195.

Izawa, M.; Kageyama, I.; Misaji, K.; Minakuchi, Y.; Sandeep, Y. (2017): Vehicle behavior analysis using linearization method of nonlinear vehicle equations of motion. *Proceeding of Society of Automotive Engineers of Japan*, pp. 1359-1364

Karnopp, D.; Crosby, M. J.; Harwood, R. A. (1974): Vibration control using semi-active force generators. *Journal of Engineering for Industry*, vol. 96, no. 2, pp. 619-626.

Ogabayashi, S. (2010): Measurement of driver's behavior and proposal of evaluation indicator of concentration on driving. *Technical Report of the Institute of Electronics, Information and Communication Engineers*, vol. 110, no. 150, pp. 37-42.

Okamoto, Y. (2010): Ride-quality assessment of automobiles by myoelectric-potential measurement. *Production Research Institute of the University of Tokyo*, vol. 62, no. 3, pp. 267-270.

Sakai, K. (2011): *Prometheus Anatomy General Atlas Anatomy General Theory/Musculoskeletal System, 2nd Edition*, pp. 236-399. IGAKU-SHOIN, Japan.

Sasaki, K. (1994): Definition and mechanism of shoulder stiffness, *Journal of All Japan Acupuncture Society*, vol. 44, no. 4.

Tao, M.; Sugimachi, T.; Suda, Y.; Shibata, K.; Katou, D. et al. (2017): A study on vehicle dynamics which can realize the motion just as intended by a driver. *Proceeding of Society of Automotive Engineers of Japan*, pp. 850-855.

Wada, N. (2012): "Running"-high-speed running of a cheetah (acinonyx jubatus). *Mammalian Science*, vol. 52, no. 1, pp. 95-101.

Watanabe, K.; Izawa, M.; Misaji, K; Takahashi, A. (2018): Using a musculoskeletal mathematical model to analyze fatigue of the muscles in the lower limbs during different motions. *Journal of Computer Modeling in Engineering and Sciences*, 2018, vol. 114, no. 2, pp. 191-207.

Yoshioka, T.; Abe, M.; Yamakado, M.; Kano, Y; Takeda, Y. et al. (2016): Analyses on vehicle dynamics improvements from human aspects with G-Vectoring control. *Proceeding of Society of Automotive Engineers of Japan*, pp. 1321-1326.

Zajac, F. E. (1989): Muscle and tendon: properties, models, scaling, and application to biomechanics and motor control. *CRC Critical Reviews of Biomedical Engineering*, vol. 17, pp. 359-411.